# Energy gaps in -graphdiyne nanoribbons

X. N. Niu, D. Z. Yang, M. S. Si, and D. S. Xue

**Articles you may be interested in**

Band-gap engineering in fluorographene nanoribbons under uniaxial strain
J. Appl. Phys. **115**, 044305 (2014); 10.1063/1.4863335

Electronic properties of graphene nanoribbons with periodically hexagonal nanoholes
J. Appl. Phys. **114**, 074307 (2013); 10.1063/1.4818615

Positional dependence of energy gap on line defect in armchair graphene nanoribbons: Two-terminal transport
and related issues
J. Appl. Phys. **114**, 034306 (2013); 10.1063/1.4813614

Band gap engineering of graphene/h-BN hybrid superlattices nanoribbons
J. Appl. Phys. **113**, 033703 (2013); 10.1063/1.4776208

Magnetic and electronic properties of -graphyne nanoribbons
J. Chem. Phys. **136**, 244702 (2012); 10.1063/1.4730325

# Energy gaps in α-graphdiyne nanoribbons

X. N. Niu, D. Z. Yang, M. S. Si,[a)] and D. S. Xue[b)]
*Key Laboratory for Magnetism and Magnetic Materials of the Ministry of Education, Lanzhou University, Lanzhou 730000, China*

α-graphdiyne is a novel predicted Dirac cone material, which is similar to graphene. But the absence of a band gap significantly limits its practical applications. In order to extend this limitation, an opening of energy gap is needed. To this end, we resort to the nanoribbon structure of α-graphdiyne. This is a conventional proposal to open up the energy gaps in nanomaterials. The results show that both the armchair and the zigzag α-graphdiyne nanoribbons do generate energy gaps, which are width-dependent. In addition, the underlying mechanism of this opening is explored. The former is ascribed to the combination of quantum confinement and edges' effect, while the latter arises from the edge magnetic ordering. These novel nanoribbons with opening energy gaps would be potentially used in electronic devices. © *2014 AIP Publishing LLC*. [http://dx.doi.org/10.1063/1.4871278]

## I. INTRODUCTION

The discovery of graphene,[1] one monolayer of carbon atoms with a honeycomb structure, has ignited intense research activities to elucidate the electronic properties of this two-dimensional (2D) electronic system. Due to the rapid progress in the preparation of graphene-related materials, infinitely many other 2D periodic carbon allotropes, including graphynes, graphdiynes, and other rectangular allotropes, can be envisioned.[2–7] Graphynes and graphdiynes are the common derivatives, which come from several acetylenic ($-C \equiv C-$) linkages introduced in graphene. It is demonstrated that these graphynes and graphdiynes are assumed to be chemically stable as $\sigma$ bond is responsible for the robustness of the lattice structure in all allotropes.[2] Indeed, finite building blocks and cuttings of these carbon allotropes have already been synthesized.[8,9] More importantly, Li *et al*. have successfully generated large area films of graphdiyne on copper surface by a cross-coupling reaction using hexaethynylbenzene.[10] This is a big step towards the preparation of extended graphynes and graphdiynes.

α-graphdiyne, another 2D layered carbon allotrope, is a new Dirac cone material.[11] In α-graphdiyne, the presence of $-C \equiv C-$ linkages will hold certain unusual phenomena, which are absent in graphene. As reported in Ref. 11, α-graphdiyne itself is a zero-gap semiconductor. To extend its practical applications, an energy gap is needed, which enables charge transport tunable externally. Although the spin-orbit coupling can open up an energy gap, the magnitude is only around $22 \times 10^{-3}$ meV.[11] Thus, other approaches should be provided to open up the energy gaps in α-graphdiyne. This can be achieved by doping,[12] transverse electric field applying,[13] and stacking.[14] Upon the cutting, an α-graphdiyne ribbon lacks the original two-dimensional periodic boundaries. The edge states are thus introduced and an opening of band gap is expected. Based on the non-equilibrium Green's function method,

electronic transport properties of nanoribbons of graphyne and its family were studied.[15,16] Just recently, Lin *et al*. investigated the electronic properties of graphdiyne nanoribbons modulated by metal adatoms.[17] However, α-graphdiyne nanoribbons have not received significant attention until now. Therefore, in order to ensure successful applications, it is desirable to explore how the peculiar structural characteristics impact energy gaps in α-graphdiyne nanoribbons.

In this work, we investigate two types of α-graphdiyne nanoribbons, called armchair and zigzag nanoribbons, through using an *ab initio* method. For each of these α-graphdiyne nanoribbons, we first carried out a geometry optimization and then calculate the energy gaps for different ribbons' width. Finally, a physical understanding to the opening of energy gaps in these α-graphdiyne nanoribbons is discussed.

The organization of this paper is as follows: a brief explanation of the computational methods is presented in Sec. II. In Secs. III and IV, we discuss the energy gaps of armchair and zigzag α-graphdiyne nanoribbons, respectively. Section V is devoted to conclusions.

## II. COMPUTATIONAL METHODS

All calculations are performed within density functional theory by using the SIESTA code.[18,19] The generalized gradient approximation correction in the form of Perdew-Burke-Ernzerhof (PBE)[20] is taken for the exchange-correction potential and the norm-conserving Troullier-Martins pseudopotentials[21] is used for the core-valence interaction. The double-$\zeta$ plus polarized atomic-orbital basis set is employed in the calculation. The mesh cutoff of 400 Ry is used. $15 \times 1 \times 1$ and $25 \times 1 \times 1$ $k$ points are chosen for the geometry optimization and the self-consistent calculation, respectively. The vacuum space is set to at least 30 Å, which is large enough to avoid the interaction between periodical images. The conjugate gradient algorithm is adopted to fully relax the structure until the maximum force on a single atom is less than 0.01 eV/Å.

a)sims@lzu.edu.cn
b)xueds@lzu.edu.cn

## III. ARMCHAIR NANORIBBONS

As a check, we first optimize the structure of α-graphdiyne. The calculated lattice constant is 14.4 Å, in agreement with the reported value of 11.42 Å.[11] In α-graphdiyne, only three typical types of bonds are emerging.[22,23] They correspond to 1.237, 1.331, and 1.395 Å, respectively. It should be noted that there is no strict single, double, or triple bond in α-graphdiyne as carbon atoms are connected through mixing $sp$ and $sp^2$ hybridizations. The band structure of α-graphdiyne shows a character of Dirac cone at K point. No electron population is observed at the Fermi level of its density of states. More importantly, the energy gap of α-graphdiyne indeed closes completely at the Dirac point in the simulations.

Similar to graphene nanoribbons (GNRs), two types of nanoribbons are obtained by cutting α-graphdiyne sheet along different directions, known as armchair and zigzag shaped edges, as illustrated in Fig. 1. To avoid edge reconstruction, the dangling σ bonds at the edges are saturated with hydrogen atoms throughout this paper. Following previous convention,[24,25] the ribbon widths are denoted by $N_a$ and $N_z$ for armchair and zigzag configurations, respectively. We refer to an α-graphdiyne armchair nanoribbon with $N_a$ lines as a $N_a$-α-AGNRs and an α-graphdiyne zigzag nanoribbon with $N_z$ zigzag chains as a $N_z$-α-ZGNRs.

Our *ab initio* calculations show that all the α-AGNRs are semiconducting and nonmagnetic, exhibiting a similar feature to GNRS.[24] Since the translational symmetry is broken in α-AGNRs compared to α-graphdiyne, an opening of energy gap is a natural consequence. In α-AGNRs, the largest energy gap is predicted to be around 0.45 eV, which is quite smaller than that of GNRs (~2.5),[24] but is comparable to that of α-graphyne nanoribbons (~0.8 eV).[26–28] This stems from the weaker hopping energies between the lattice sites in α-graphdiyne.[11]

The gap of $N_a$-α-AGNRs is inversely proportional to its width, as displayed in Fig. 2. More importantly, the variations of energy gaps are separated into three distinct families, which are as $N_a = 3p$, $3p + 1$, $3p + 2$ with $p$ being a nonnegative integer. The gap behaves a hierarchy as $\Delta_{3p+1} > \Delta_{3p} > \Delta_{3p+2}$, as shown in Fig. 2(a). The band structures for $N_a = 11$, 12, and 13 are shown in Fig. 2(b), suggesting that the α-AGNRs are direct semiconductors at Γ point. Since the α-graphdiyne itself is a gapless semiconductor,[11] quantum confinement is the first factor to dominate the semiconducting behavior of α-AGNRs. Moreover, this quantum confinement can be characterized by $\Delta_{N_a} \propto w_a^{-1}$. The solid curves in Fig. 2(a) are obtained through fitting the above quantum confinement. Another factor ascribed to the appearance of the energy gaps in α-AGNRs is the edges' effect. This can be characterized by the variation of carbon bond lengths at edges, which are shortened by around 0.8%–1.0% for the 11-, 12-, and 13-α-AGNRs as compared to those in the middle of the ribbon.

## IV. ZIGZAG NANORIBBONS

In the case of α-ZGNRs, with nonmagnetic (NM) ordering between two edges, there is no energy gap as the upper and lower bands are degenerate at the Fermi level. In Fig. 3(a), the edge states are completely localized at $E_F$ and close to the X point, in agreement with GNRs[24] and other graphyne/graphdiyne nanoribbons.[26–28] The almost flat bands near the Fermi level are expected to give rise to a remarkable sharp peak in the density of states, where the charge density is extremely localized on the edge states. Due
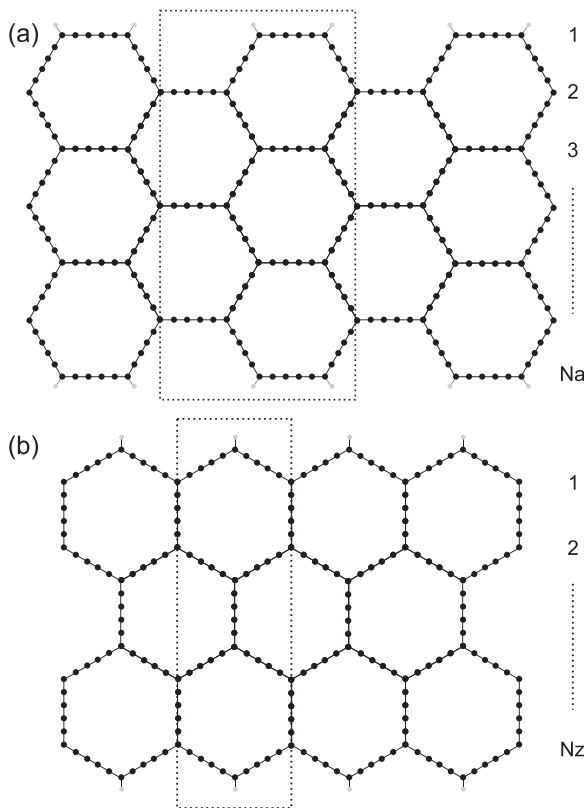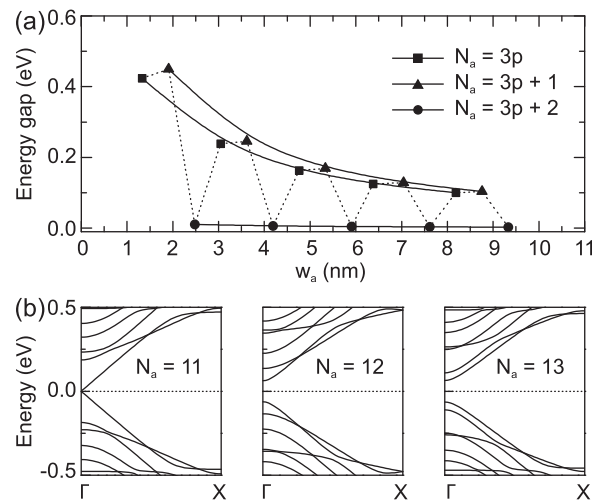


FIG. 1. Schematics of (a) armchair and (b) zigzag α-graphdiyne nanoribbons. The unit cell is delimited by the dashed lines. The edge carbon atoms are saturated with hydrogen atoms. $N_a$ and $N_z$ identify the width of armchair and zigzag nanoribbons, respectively.



FIG. 2. (a) The variation of energy gaps of $N_a$-α-AGNRs as a function of width from *ab initio* calculations (symbols). The solid lines are fit from the quantum confinement $\Delta_{N_a} \propto w_a^{-1}$. (b) Band structures of $N_a$-α-AGNRs with $N_a = 11$, 12, and 13.
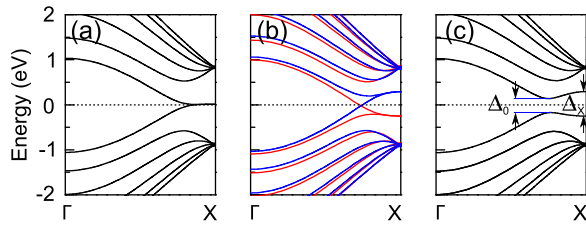
FIG. 3. Band structures of 6-α-ZGNRs for the spin confinements between two edges: (a) NM, (b) FM, and (c) AFM. The red (blue) curves represent the spin up (spin down) states. The Fermi energy level is set to 0 eV. $\Delta_0$ and $\Delta_X$ respectively represent the direct band gap and the one at the high symmetry X point with the AFM spin configuration.



FIG. 5. The variation of $\Delta_X$ and $\Delta_0$ as a function of the width for α-ZGNRs with the AFM spin confinement between two edges.

to the strong tight-binding character of these edge states, the Coulomb energies are very large, resulting in spin-polarized edges. This should be the origin of magnetic ordering in α-ZGNRs[31] (discussed as below). This is slightly different from the magnetism induced by vacancies,[32,33] where the dangling bonds play a vital role.

Upon inclusion of spin polarization, a remarkable new feature arises in the band structure. The α-ZGNRs are predicted to be metallic with ferromagnetic (FM) ordering between two edges. Meanwhile, it has a direct change on its band structure, as shown in Fig. 3(b). The edge states are spin-splitting as one is above $E_F$ and the other is below $E_F$. Thus, the original localized edge states are now spin-polarized, with only the spin up states being filled. This also can be explicitly observed in the corresponding spin distributions where the edge atoms are spin up, as displayed in Fig. 4(a). This FM spin configuration is more stable by around 26.9 meV than that of NM in the case of 6-α-ZGNRs. The energy difference between NM and FM states decreases as the width of nanoribbons increases. If two edges are antiferromagnetic (AFM) coupling, it generates the semiconducting ground state, as displayed in Fig. 3(c). It is more stable by about 30.4 meV than that of NM coupling in the case of 6-α-ZGNRs. Thus, AFM coupling is the ground state of α-ZGNRs. The spin

distributions of 6-α-ZGNRs with the AFM spin configuration is given in Fig. 4(b). The magnetic moment localized on the edge atom is about 0.11 $\mu_B$, which is smaller than the value of GRNs ($\sim$0.55$\mu_B$),[34] but is comparable to that of graphyne/graphdiyne nanoribbons ($\sim$0.15$\mu_B$).[26,30] It is important to note that the atomic magnetic moment spreads from the edge to the center of the ribbon with a notable decay. This is because the flat subband or the edge states are formed in these nanoribbons (see Fig. 3(a)).

Two types of energy gaps $\Delta_0$ and $\Delta_X$ (Fig. 3(c)) are detected in α-ZGNRs, which originate from the staggered sublattice potentials.[29] Since the strength of the staggered potentials in the middle of the ribbons decreases as the width increases, the band gaps of α-ZGNRs are inversely proportional to the width as shown in Fig. 5. The energy gaps $\Delta_X$ remains nearly unchanged as the width of α-ZGNRs increases, while the energy gaps $\Delta_0$ drops sharply as the width increases. The averaged gaps of $\Delta_0$ and $\Delta_X$ from nanoribbons' width $N_z = 2$ to $N_z = 14$ are about 0.14 and 0.27 eV, respectively. Both of them are quite smaller than those values (0.3 and 0.5 eV) of GNRs.[24]

## V. CONCLUSIONS

In conclusion, we have studied the energy gaps of α-graphdiyne nanoribbons, with two typical edges, using *ab initio* methods. The results shown that either armchair or zig-zag shaped edges generate energy gaps which decreases as the ribbon widths increase. The former has a energy gap caused by the quantum confinement and the edges' effect, while the latter arises from the edge magnetic ordering. These nanoribbons with opening up energy gaps would be potential used in electronic applications.
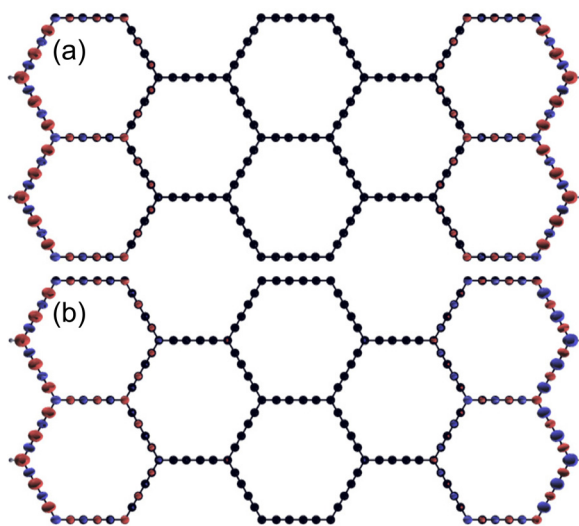
## ACKNOWLEDGMENTS

FIG. 4. Spin distributions of the (a) FM and (b) AFM states. The red and blue isosurfaces stand for the spin-up and spin-down states, respectively. The isovalue is set to 0.002 $e$/Å$^3$. The black and white balls represent carbon and hydrogen atoms, respectively.
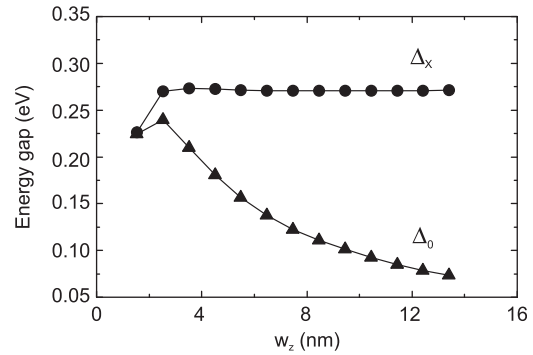
[1]K. S. Novoselov, A. K. Geim, S. V. Morozov, D. Jiang, Y. Zhang, S. V. Dubonos, I. V. Grigorieva, and A. A. Firsov, Science **306**, 666 (2004).

[2] A. H. Castro Neto, F. Guinea, N. M. R. Peres, K. S. Novoselov, and A. K. Geim, Rev. Mod. Phys. **81**, 109 (2009).

[3] A. A. Balandin, Nature Mater. **10**, 569 (2011).

[4] J. M. Kehoe, J. H. Kiley, J. J. English, C. A. Johnson, R. C. Petersen, and M. M. Haley, Org. Lett. **2**(7), 969 (2000).

[5] M. M. Haley, Pure Appl. Chem. **80**, 519 (2008).

[6] T. Yoshimura, A. Inaba, M. Sonoda, K. Tahara, Y. Tobe, and R. V. Williams, Org. Lett. **8**(14), 2933 (2006).

[7] D. Z. Yang, M. S. Si, G. P. Zhang, and D. S. Xue, "Crystal momentum-dependent anisotropy of Dirac cone in the rectangular carbon allotropes," Europhys. Lett. (to be published).

[8] F. Diederich, Nature (London) **369**, 199 (1994).

[9] U. H. F. Bunz, Y. Rubin, and Y. Tobe, Chem. Soc. Rev. **28**, 107 (1999).

[10] G. Li, Y. Li, H. Liu, Y. Guo, Y. Li, and D. Zhu, Chem. Commun. **46**, 3256 (2010).

[11] X. Niu, X. Mao, D. Yang, Z. Zhang, M. Si, and D. Xue, Nanoscale Res. Lett. **8**, 469 (2013).

[12] M. Roya, Nano **8**, 135006 (2013).

[13] J. Kang, F. Wu, and J. Li, J. Phys.: Condens. Matter **24**, 165301 (2012).

[14] O. Leenaerts, B. Partoens, and F. M. Peeters, Appl. Phys. Lett. **103**, 013105 (2013).

[15] Y. Jing, G. Wu, L. Guo, Y. Sun, and J. Shen, Comput. Mater. Sci. **78**, 22–28 (2013).

[16] W. Wu, W. Guo, and X. C. Zeng, Nanoscale **5**, 9264–9276 (2013).

[17] Z.-Z. Lin, Q. Wei, and X. Zhu, Carbon **66**, 504–510 (2014).

[18] P. Ordejón, E. Artacho, and J. M. Soler, Phys. Rev. B **53**, R10441 (1996).

[19] J. M. Soler, E. Artacho, J. D. Gale, A. García, J. Junquera, P. Ordejón, and D. Sánchez-Portal, J. Phys.: Condens. Matter **14**, 2754 (2002).

[20] J. P. Perdew, K. Burke, and M. Ernzerhof, Phys. Rev. Lett. **77**, 3865 (1996).

[21] N. Troullier and J. Martins, Solid State Commun. **74**, 613 (1990).

[22] B. G. Kim and H. J. Choi, Phys. Rev. B **86**, 115435 (2012).

[23] Q. Yue, S. Chang, J. Kang, J. Tan, S. Qin, and J. Li, J. Phys. Chem. C **117**, 14804 (2013).

[24] Y.-W. Son, M. L. Cohen, and S. G. Louie, Phys. Rev. Lett. **97**, 216803 (2006).

[25] M. Ezawa, Phys. Rev. B **73**, 045432 (2006).

[26] Q. Yue, S. Chang, J. Kang, J. Tan, S. Qin, and J. Li, J. Chem. Phys. **136**, 244702 (2012).

[27] L. D. Pan, L. Z. Zhang, B. Q. Song, S. X. Du, and H.-J. Gao, Appl. Phys. Lett. **98**, 173102 (2011).

[28] N. Narita, S. Nagai, S. Suzuki, and K. Nakao, Phys. Rev. B **58**, 11009 (1998).

[29] C. L. Kane and E. J. Mele, Phys. Rev. Lett. **95**, 146802 (2005).

[30] G. Yu, Z. Liu, W. Gao, and Z. Zheng, J. Phys.: Condens. Matter **25**, 285502 (2013).

[31] S. Okada and A. Oshiyama, Phys. Rev. Lett. **87**, 146803 (2001).

[32] M. S. Si, J. Y. Li, H. G. Shi, X. N. Niu, and D. S. Xue, Europhys. Lett. **86**, 46002 (2009).

[33] D. Gao, J. Zhang, G. Yang, J. Qi, M. Si, and D. Xue, J. Phys. Chem. C **115**, 16405–16410 (2011).

[34] L. Pisani, J. A. Chan, B. Montanari, and N. M. Harrison, Phys. Rev. B **75**, 064418 (2007).